

**Supplemental information**

**The zebrafish heart harbors  
a thermogenic beige fat depot analog  
of human epicardial adipose tissue**

**Paul-Andres Morocho-Jaramillo, Ilan Kotlar-Goldaper, Bhakti I. Zakarauskas-Seth, Bettina Purfürst, Alessandro Filosa, and Suphansa Sawamiphak**

Supplemental Information

Supplementary Figures

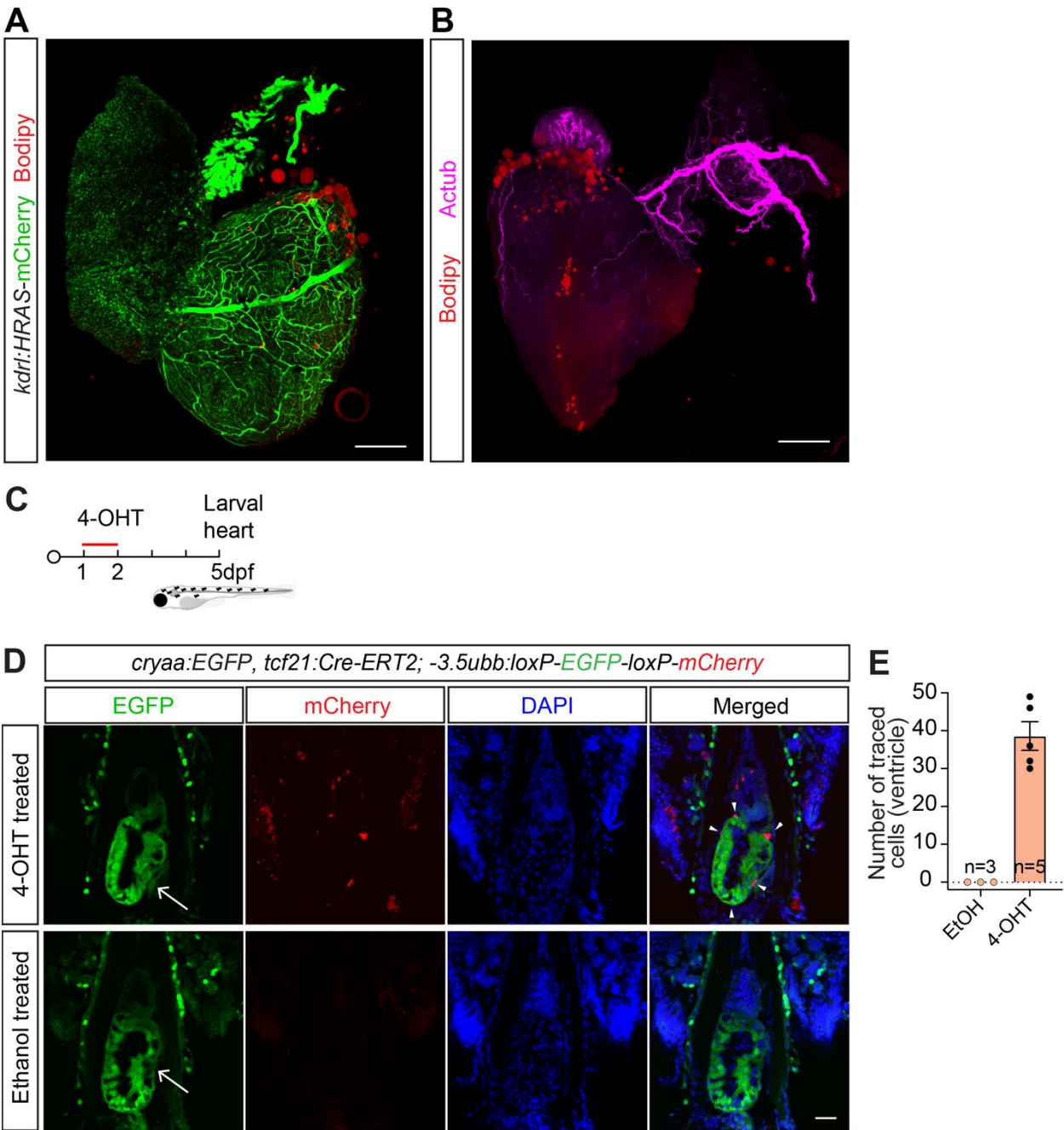
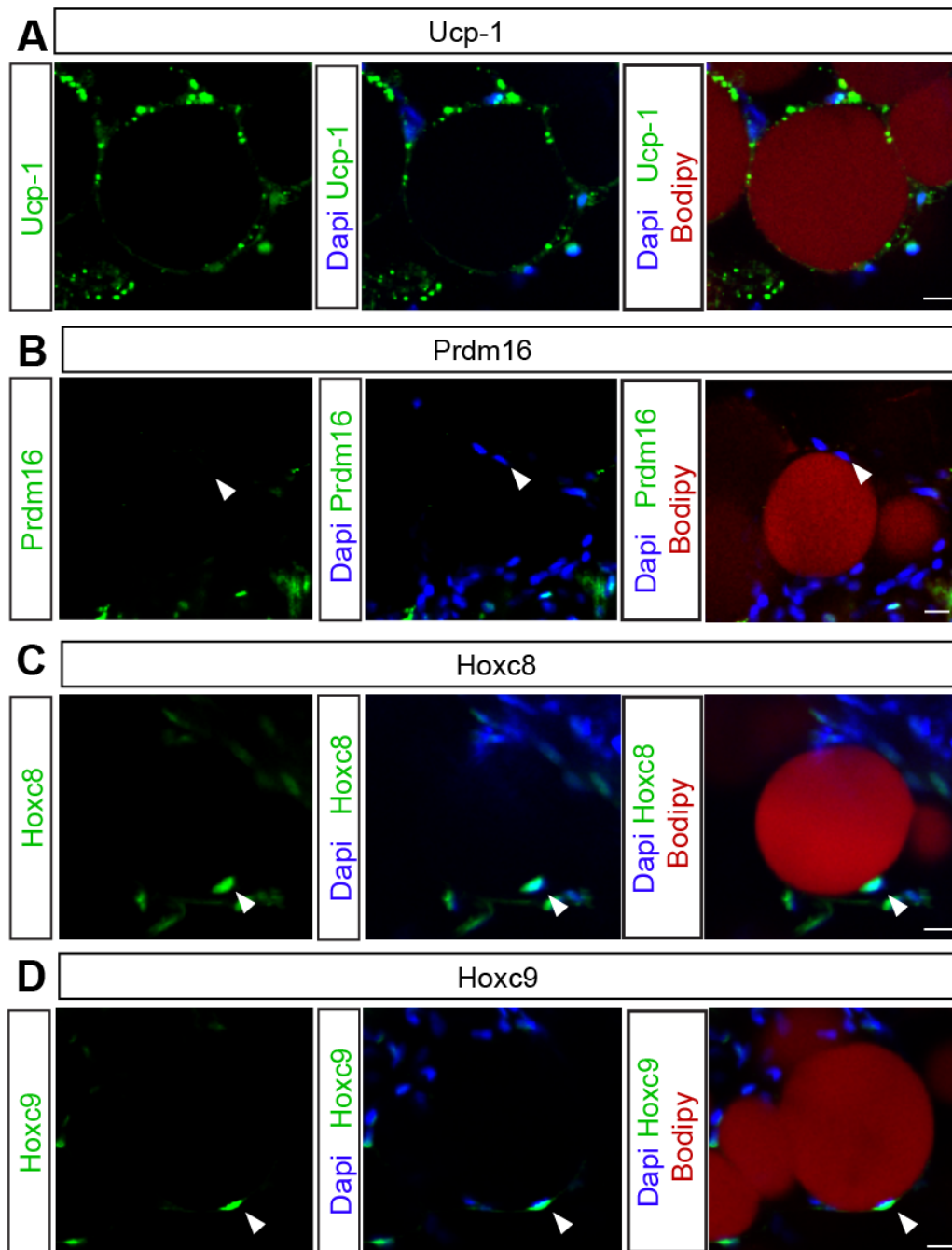
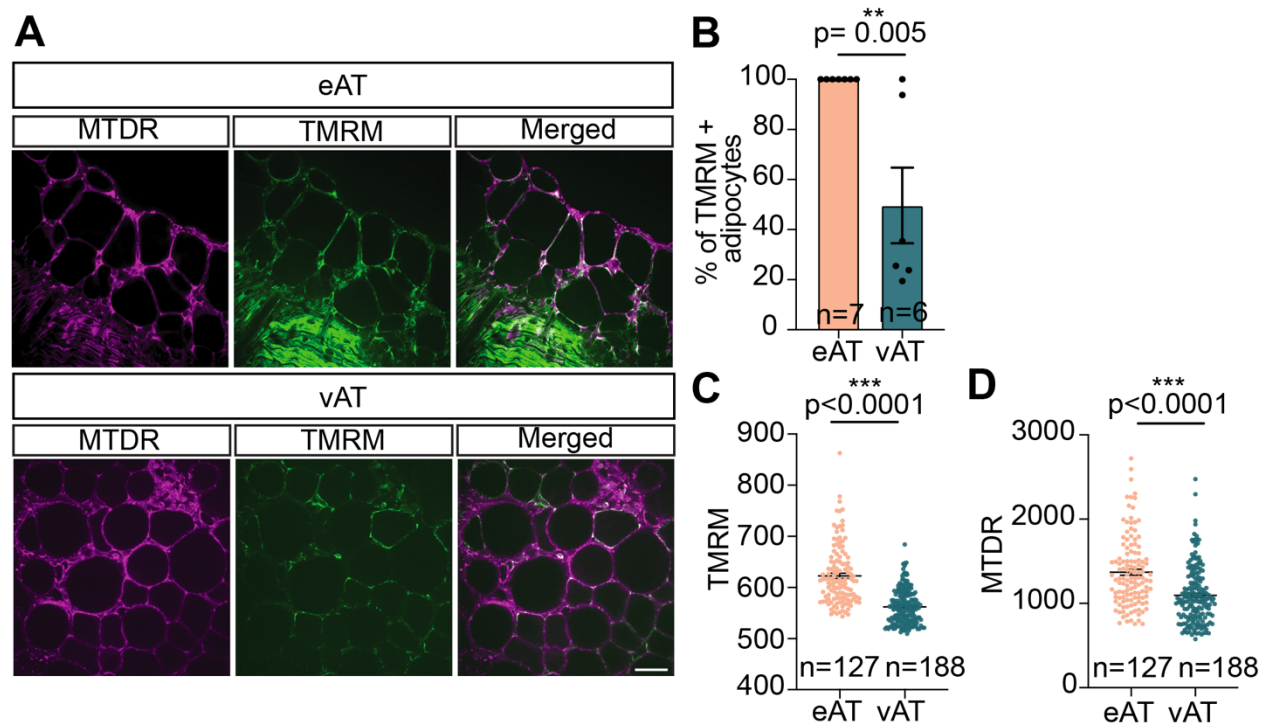


Figure S1 (related to Figure 1). Localization and lineage tracing of epicardial adipocytes in zebrafish. (A) Z-projection of a *kdrl:HRAS-mCherry* zebrafish heart,

showing vascularization of adipose tissue with coronary vessels, visualized by Bodipy staining and mCherry immunostaining, respectively. Scale bar, 200  $\mu$ m. **(B)** Z-projection of a zebrafish heart, in which autonomic nerves and adipocytes were visualized by immunofluorescent staining of acetylated tubulin (Actub) and staining with Bodipy. Scale bar, 200  $\mu$ m. **(C)** Schematic illustration of Cre-mediated pulse-chase lineage tracing of Tcf21+ proepicardial cells. **(D)** *cryaa:EGFP; tcf21:Cre-ERT2; ubb:loxP-EGFP-loxP-mCherry* larval hearts (arrows), treated with 4-hydroxy tamoxifen (4-OHT) and ethanol at 1-2 dpf. Ubiquitous expression of EGFP and tcf21-derived mCherry expressing cells (arrowheads) were examined by immunofluorescent staining at 5 dpf. Scale bar 30  $\mu$ m. **(E)** Bar graph showing numbers of *tcf21:Cre-ERT2*-traced cells in the ventricle at 5 dpf. Data are presented as mean  $\pm$  S.E.M. n indicates number of animals.



**Figure S2 (related to Figure 2). Expression of white and brown adipocyte markers in zebrafish epicardial adipocytes. (A-D)** Confocal images of whole-mounted zebrafish hearts, immunostained for Ucp1, Prdm16, Hoxc8, and Hoxc9, and stained with BODIPY 558/568 C12 and DAPI. White arrowheads indicate nuclear localization of the proteins in adipocytes. Scale bar, 10  $\mu$ m.



**Figure S3 (related to Figure 2). Higher content of active mitochondria in zebrafish eAT, as compared to white adipose tissue. (A)** Confocal images showing epicardial adipose tissue (eAT) and abdominal visceral adipose tissue (vAT) explants, in which active mitochondria were labelled with mitotracker deep red (MTDR) and Tetramethylrhodamine, methyl ester (TMRM). Scale bar, 50  $\mu$ m. **(B)** Bar graph depicting lower percentages of TMRM-positive adipocytes in vAT explants. **(C, D)** Bar graphs depicting lower densities of TMRM **(C)** and MTDR **(D)** positive mitochondria in eAT and vAT adipocytes. n indicates number of animals in (B) or number of analyzed adipocytes from five fish per condition in **(C, D)**. Data are presented as mean  $\pm$  S.E.M.  $**p < 0.01$ ,  $***p < 0.001$ , two-tailed t-test. n indicates number of animals.

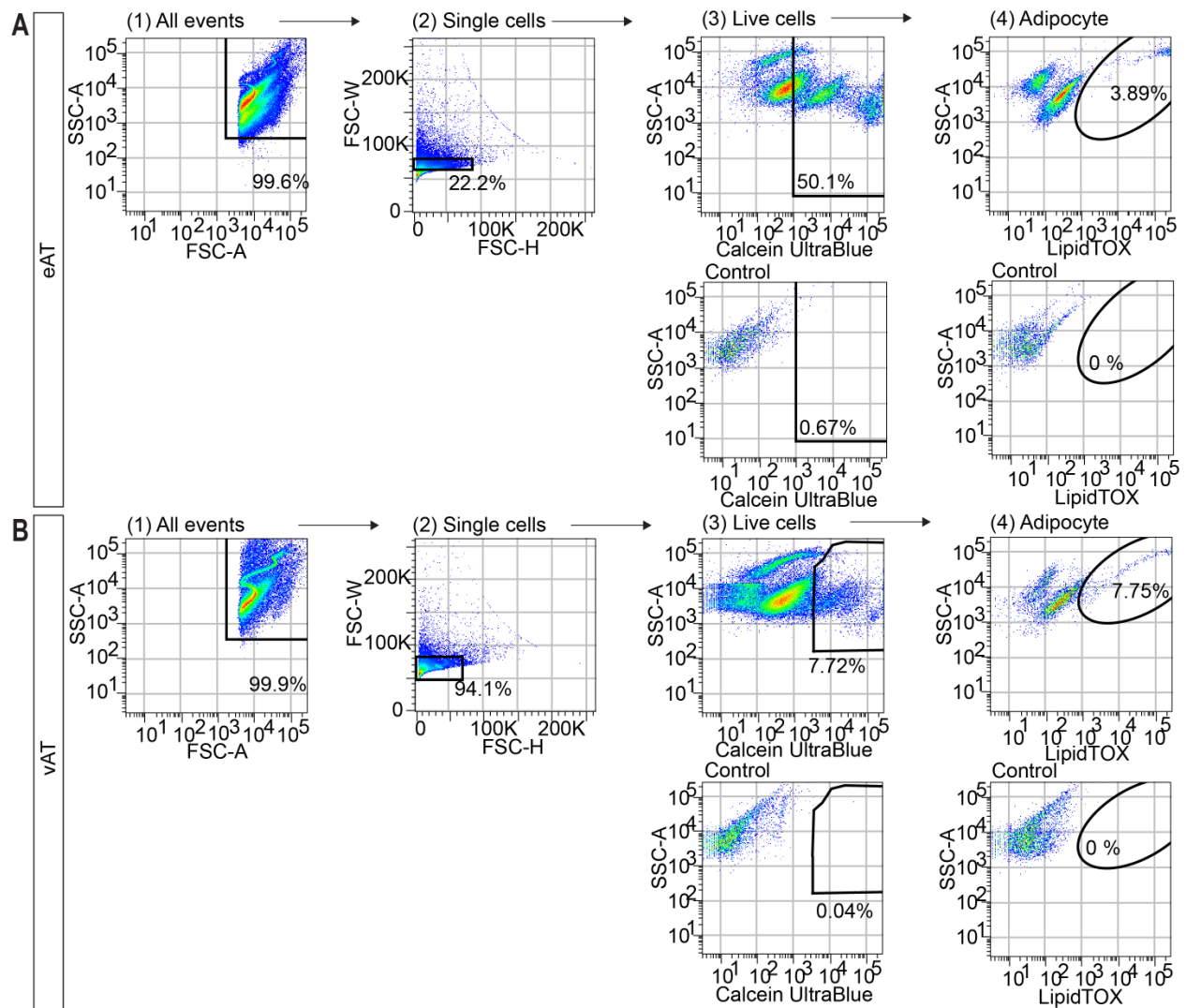


**Figure S4 (related to Figure 3). Gating strategy of adipocytes. eAT (A) and vAT (B)** were isolated by flow cytometry for analysis of thermogenesis activity by ErthermAC.

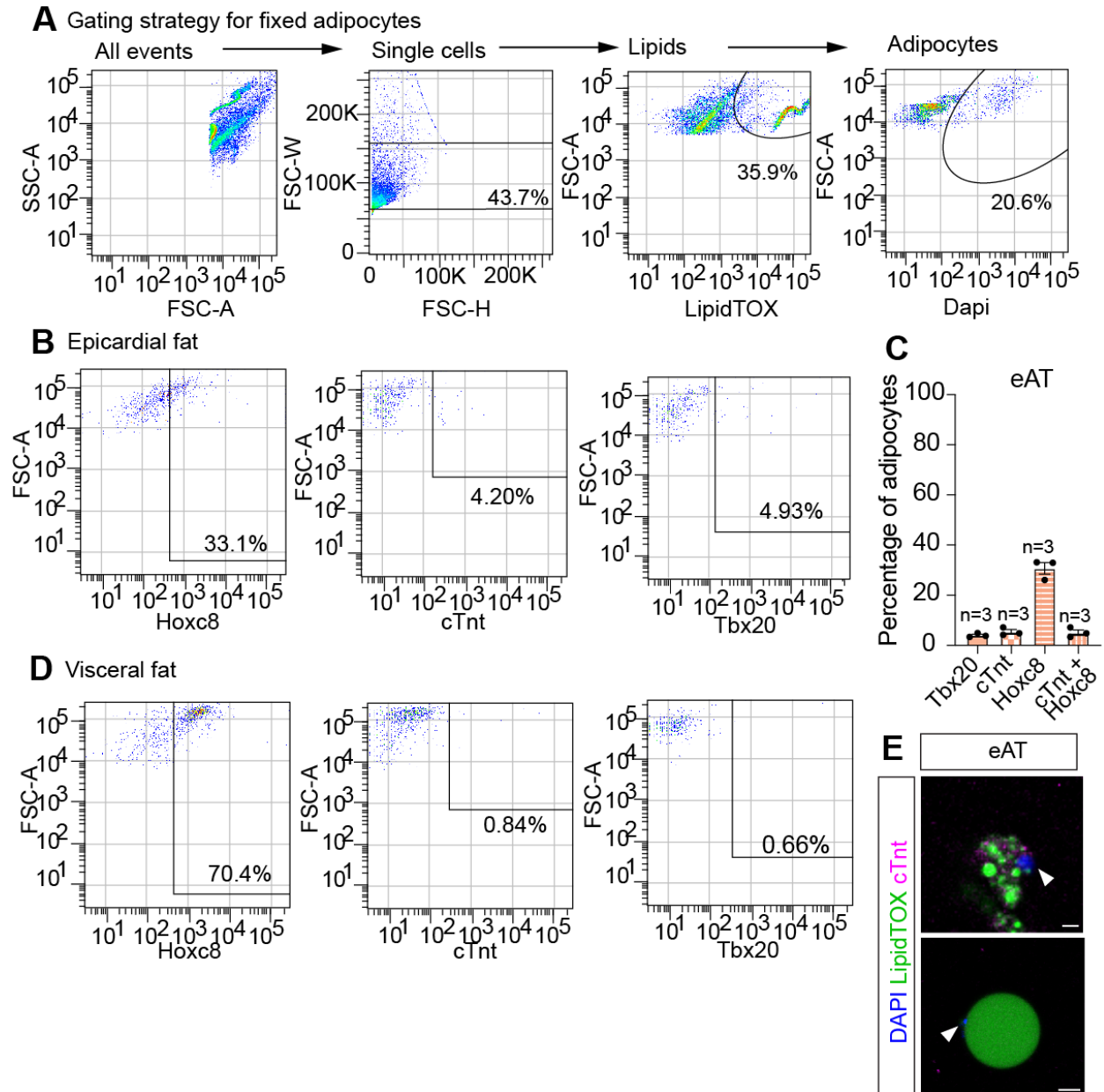


**Figure S5 (related to Figure 4). Assessment of cardiac development and homeostasis gene expression in epicardial adipocytes by flow cytometry and immunofluorescence. (A and B)** Subpopulations of adipocytes from epicardial fat, labelled with LipidTox and DAPI **(A)** express Hoxc8, cTnt, and Tbx20 **(B)**. **(C)** Bar graph depicting percentages of Hoxc8+, cTnt+, Tbx20+, and cTnt+Hoxc8+ per total adipocytes in the eAT. Data are presented as mean  $\pm$  S.E.M. n indicates number of animals. **(D)**

Majority of vAT adipocytes were Hoxc8+, but did show detectable cTnt or Tbx20 expression. **(E)** Representative images of dissociated epicardial adipocytes, visualized by lipidTox accumulation, some of which express cTnt, detected by immunofluorescent staining. Arrowheads indicate adipocyte nuclei. Scale bar, 4  $\mu$ m. Upper panel showed epicardial adipocyte co-expressed cTnt. cTnt was not detectable in adipocyte shown in the lower panel. White arrowheads indicates adipocyte nuclei labelled with DAPI.



## Genes shown in Figure 5D

## ■ upregulated in human and zebrafish eAT (top20)

human_ID	zebrafish_ID	human_log2FC	zebrafish_log2FC
ENSG00000164532	ENSDARG00000005150	10,2211	9,3887
ENSG00000130700	ENSDARG000000017821	7,8020	1,9722
ENSG00000183421	ENSDARG000000043211	5,1737	0,4910
ENSG00000188176	ENSDARG000000055632	4,5488	4,2133
ENSG00000147573	ENSDARG000000058158	4,0264	8,7259
ENSG00000101311	ENSDARG000000052652	3,9087	0,2258
ENSG00000118526	ENSDARG000000036869	3,8240	2,4209
ENSG00000096696	ENSDARG000000076673	3,4611	1,7242
ENSG00000153820	ENSDARG000000017429	3,4018	4,8271
ENSG00000117707	ENSDARG000000055158	3,3991	1,6897
ENSG00000124772	ENSDARG000000070919	3,3840	4,3632
ENSG00000215218	ENSDARG000000079276	3,2513	7,1007
ENSG00000079931	ENSDARG000000031136	2,9777	3,5533
ENSG00000105509	ENSDARG000000042983	2,9573	5,1667
ENSG00000169071	ENSDARG000000076227	2,8838	3,2004
ENSG00000167971	ENSDARG000000046107	2,7586	0,9878
ENSG00000103888	ENSDARG000000039881	2,6991	1,8262
ENSG00000106278	ENSDARG000000020871	2,5553	4,1617
ENSG00000141639	ENSDARG0000000110581	2,5456	1,6705
ENSG00000162631	ENSDARG000000073713	2,4122	0,2522

## ■ upregulated in human sAT and zebrafish vAT(top20)

human_ID	zebrafish_ID	human_log2FC	zebrafish_log2FC
ENSG00000037965	ENSDARG000000070346	-8,9036	-9,1642
ENSG00000180806	ENSDARG000000092809	-7,3938	-7,6380
ENSG00000120068	ENSDARG000000056027	-6,4626	-3,2247
ENSG00000170689	ENSDARG000000056023	-5,1066	-2,7830
ENSG00000106004	ENSDARG000000102501	-4,6856	-4,3149
ENSG00000131771	ENSDARG000000076280	-4,3914	-0,9056
ENSG00000145824	ENSDARG000000056627	-3,6315	-3,9584
ENSG00000155966	ENSDARG000000052242	-2,9630	-1,5614
ENSG00000175161	ENSDARG000000062633	-2,8711	-6,6697
ENSG00000185818	ENSDARG000000077256	-2,4250	-3,0299
ENSG00000141449	ENSDARG000000039196	-2,2469	-4,0214
ENSG00000130876	ENSDARG000000008100	-2,1133	-2,3330
ENSG00000170786	ENSDARG000000016233	-2,0903	-1,8126
ENSG00000079689	ENSDARG000000058732	-1,9503	-1,1526
ENSG00000162444	ENSDARG000000070486	-1,9401	-1,7417
ENSG00000124003	ENSDARG000000086481	-1,8104	-1,9932
ENSG00000158516	ENSDARG000000043722	-1,7426	-17,3074
ENSG00000105088	ENSDARG000000102825	-1,6073	-0,8890
ENSG00000278535	ENSDARG000000004141	-1,4856	-3,7050
ENSG00000010319	ENSDARG000000007560	-1,4552	-2,0455

## ■ upregulated in human eAT but downregulated in zebrafish eAT (top20)

human_ID	zebrafish_ID	human_log2FC	zebrafish_log2FC
ENSG00000081052	ENSDARG000000002831	4,0948	-0,8197
ENSG00000151224	ENSDARG000000039605	4,0894	-9,0946
ENSG00000078725	ENSDARG000000078302	3,7369	-0,1313
ENSG00000112486	ENSDARG000000038968	3,7304	-4,6057
ENSG00000154113	ENSDARG000000068181	3,7074	-1,3552
ENSG00000166922	ENSDARG000000032126	3,5769	-1,7886
ENSG00000109072	ENSDARG000000053831	3,4093	-4,0363
ENSG00000156510	ENSDARG000000038703	3,3469	-2,3410
ENSG00000276418	ENSDARG000000061713	3,3404	-2,5828
ENSG00000099958	ENSDARG000000033871	3,1524	-2,4378
ENSG00000106018	ENSDARG000000012353	2,9349	-6,6642
ENSG00000154639	ENSDARG000000043658	2,8708	-1,4678
ENSG00000172367	ENSDARG000000040568	2,6993	-4,1138
ENSG00000162366	ENSDARG000000017127	2,6565	-0,9768
ENSG00000160183	ENSDARG000000036545	2,6512	-4,3100
ENSG00000129354	ENSDARG000000096454	2,5621	-4,3596
ENSG00000099960	ENSDARG000000068286	2,5420	-4,3945
ENSG00000164142	ENSDARG000000061021	2,4855	-0,2819
ENSG00000005513	ENSDARG000000037782	2,4663	-5,5458
ENSG00000178882	ENSDARG000000023484	2,4145	-1,5737

## ■ upregulated in zebrafish eAT but downregulated in human eAT (top20)

human_ID	zebrafish_ID	human_log2FC	zebrafish_log2FC
ENSG00000170549	ENSDARG000000101831	-5,7771	6,1882
ENSG00000170561	ENSDARG000000001785	-4,2691	2,2609
ENSG00000143320	ENSDARG000000030449	-3,2008	2,5615
ENSG00000075035	ENSDARG000000061819	-2,8542	3,3995
ENSG00000004939	ENSDARG000000012881	-2,8294	4,6586
ENSG00000164708	ENSDARG000000057571	-2,7617	10,9069
ENSG00000150893	ENSDARG000000102626	-2,7473	3,6225
ENSG00000176842	ENSDARG000000034043	-2,4764	2,8443
ENSG00000134317	ENSDARG000000061391	-1,9848	2,1631
ENSG00000085741	ENSDARG000000014796	-1,9316	6,6748
ENSG00000133110	ENSDARG000000043806	-1,8503	8,2995
ENSG00000169047	ENSDARG000000054087	-1,7975	1,8073
ENSG00000166165	ENSDARG000000043257	-1,5554	2,1312
ENSG00000153162	ENSDARG000000015686	-1,4321	2,8131
ENSG00000158458	ENSDARG000000077818	-1,3634	1,7280
ENSG00000089225	ENSDARG000000024894	-1,2430	8,6155
ENSG00000035664	ENSDARG000000061096	-1,2353	3,6422
ENSG00000172572	ENSDARG000000004227	-1,2172	2,9232
ENSG00000166148	ENSDARG000000045788	-1,1960	2,4579
ENSG00000285854	ENSDARG000000019644	-1,1676	4,3786

**Figure S6 (related to Figure 5). Top 20 most differentially expressed genes in young zebrafish and aged human eAT, as compared to classical white adipose tissues, identified by RNA sequencing (RNA-Seq). Fold changes of all orthologues, indicated by Ensembl gene IDs, are displayed as log base 2 values.**

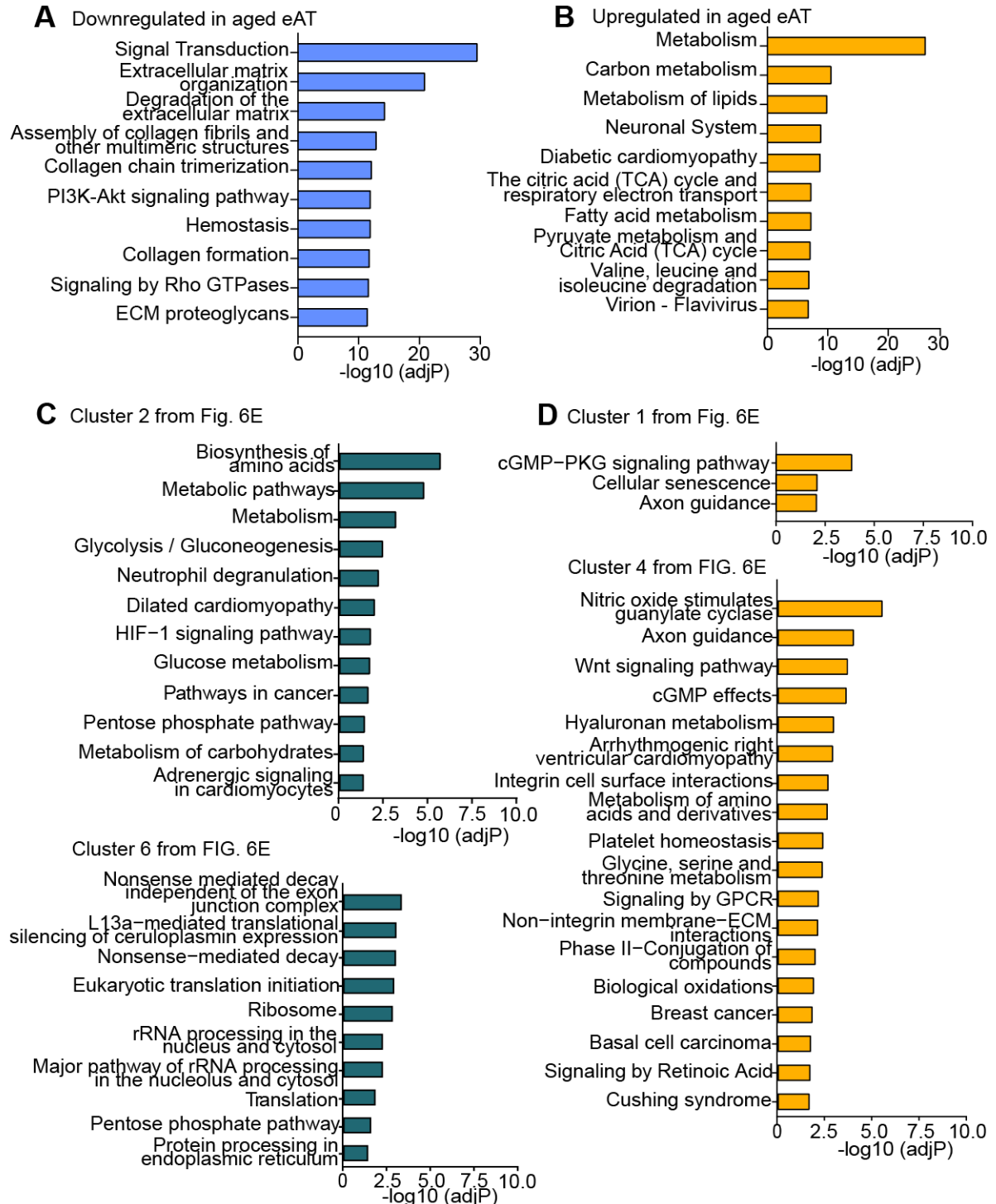


**Figure S7 (related to Figure 6). Highly represented pathways of up- and downregulated genes from cross-species analysis of whole transcriptomic profile**

**of eAT. (A and B)** Enriched pathways associated with downregulated **(A)** and upregulated **(B)** genes in aged as compared to young mouse eAT. **(C and D)** Significantly overrepresented pathways based on gene clusters with similar expression in human and zebrafish (cluster 2 and 6 from Fig. 6E) **(C)** or those with similar expression in human and mouse (cluster 1 and 4 from Fig. 6E) **(D)**. All pathway enrichment analyses were done using KEGG and REACTOME databases. Enrichment is expressed as the  $-\log[P]$  adjusted for multiple comparisons. Only DEGs with log2 fold change score more than 0.6 were included in the analysis.